10 micron mapping of Jupiter on the CFHT after the impacts of comet P/Shoemaker-Levy 9

F. Billebaud, P. Drossart, I. Vauglin, P. Merlin, F. Sibille, Philippe Lognonné, E. Lellouch, B. Mosser

GEOPHYSICAL RESEARCH LETTERS, VOL. 22, NO. 13, PAGES 1777-1780, JULY 1, 1995

10 Micron Mapping of Jupiter on the CFHT after the Impacts of Comet P/Shoemaker-Levy 9

F. Billebaud,[1] P. Drossart,[2] I. Vauglin, [3] P. Merlin,[3] F. Sibille,[3] P. Lognonné,[4] E. Lellouch[2] and B. Mosser[5]

Abstract. We have observed Jupiter on July 24, 25, 26 and 27, 1994, in thermal infrared, using the French National 10 micron array camera "C10μ", mounted on the Canada-France-Hawaii 3.6 meter telescope. The observations were made using both broad-band and narrow-band filters, as well as a Circular Variable Filter (CVF). Two observing programs were scheduled, one concerning atmospheric observations and the other one focusing on seismological observations (*Lognonné et al.*, 1994). We present here preliminary results concerning the atmospheric program. The main result is that persistent brightness temperature enhancements still exist several days after the impacts at several wavelengths, corresponding to a long term perturbation associated to the impact sites.

Introduction

We have recorded images of Jupiter in the 10 micron atmospheric window, shortly after the impacts of the comet P/Shoemaker-Levy 9. The camera we used is equipped with a 64×64 Si:Ga array detector, sensitive in the 4 to 17 μm range and optimized for ground-based observations in the mid-infrared window, which was developped by the Equipe Infrarouge of the Observatoire de Lyon, France. The camera comprises 10 broad and narrow-band filters, and two Circular Variable Filters (CVFs), covering the range 4.4 to 7.85 μm and 7.72 to 13.64 μm, with a spectral resolution of 50 at 10 μm. Two focal scales are also available, with a spatial sampling of 0.5 or 0.8 arcsec per pixel.

The atmosphere dedicated observations were made using the 7.72-13.64 μm CVF at several precise wavelengths. Due to bad meteorological conditions, observations could not start before July 24. CVF sequences were made on July 25, 26 and 27, with a spatial sampling of 0.8 arcsec per pixel, which allowed us to have the entire disk of the planet on the mosaic (the size of Jupiter was between 35 and 38 arcsec in diameter at that time). To cope with the short amount of observing time available for our program, we selected 6 CVF positions, centered at: 7.93 μm (P branch of the ν_4 emission band of Methane), 8.55 μm (continuum near the ν_4 emission band of Methane), 11.36 μm (ammonia continuum near the ν_9 emission band of ethane), 12.18 μm (ν_9 emission band of ethane), 13.33 μm (continuum between the ν_9 emission band of ethane and the ν_5 emission band of acetylene) and 13.60 μm (Q branch of the ν_5 emission band of acetylene).

Data reduction

In the mid-infrared (7 to 14 μm), sky and background emissions are so important that special observing techniques are necessary. For this reason, all our images were recorded in a "chopping + nodding" mode. The chopping period was of about 500 msec, while the nodding period was of about 1-2 min. With the chopping, the contribution of the sky is subtracted to all individual frames which are then flat-fielded. All the chopped images for a single position of nodding are after that co-added and averaged. The same process is applied to the other position of nodding, both resulting images being then averaged. The signal obtained is thus flat-fielded and corrected for contributions from the sky and all background emissions.

In order to improve the signal to noise ratio of the CVF images, it appeared necessary to co-add corrected images. This was done for images recorded continuously in time, on sequences never exceeding 10 minutes at the maximum. This usually represents sequences of 4 to 7 images, depending on the integration time per frame and on the number of chopping and nodding cycles. The upper limit of 10 minutes has been imposed arbitrarily as the "maximum acceptable degradation of the spatial resolution". It corresponds to a spreading of slightly less than 2.5 pixels at the equator of Jupiter (1.97 arcsec) and of about 1.8 pixels at the latitude of -43 deg (1.44 arcsec). This gives us a set of 18 CVF images for July 25, 26 for July 26 and 12 for July 27, each of these images corresponding to the sum of several hundreds to several thousands of individual frames. These "final" images have then been deconvolved. We used the calibration star images to determine the Point Spread Function (PSF) of the instrument. The PSF

[1]Space Science Department of the European Space Agency, ESTEC, Noordwijk, The Netherlands

[2]DESPA, Observatoire de Paris, Meudon, France

[3]Observatoire de Lyon, Saint Genis-Laval, France

[4]Institut de Physique du Globe, Laboratoire de Sismologie, Paris, France

[5]Institut d'Astrophysique, Paris, France

Paper number 95GL01438
0094-8534/95/95GL-01438$03.00

may vary from night to night, but is constant with the wavelength. The deconvolution technique was the same for all images, every night.

Interpretation and discussion

Depending on the observed wavelength, different levels of the atmosphere are probed, all being located in the upper troposphere and the stratosphere of Jupiter. By comparison with the Voyager IRIS data (Kunde et al., 1982), we have made an estimate of the atmospheric levels we preferentially probe with our CVF observations: around 30 mbar and above at 7.93 μm, between 0.5 and 1 bar at 8.55 μm, around 0.5 bar at 11.36 and 13.33 μm and between 10 and 100 mbar at 12.18 and 13.60 μm. As these estimates were obtained considering mainly the levels where the optical depth is about 1, there will obviously be a contribution from levels immediately above and below the ones we mention, which could be important. In particular, these estimates were made considering the atmosphere of Jupiter as "unperturbed", therefore it is possible that the perturbation by the impacts has changed the sounded altitude and that a strong stratospheric emission would be seen at almost all mid-infrared wavelengths.

Our set of images exhibits two impact site complexes: the G-S-D-R-Q2 site near 30 degrees of longitude (System III) and the U-K-W one near 275 degrees. The global uncertainty on the calibration of the July 25 and 26 images is estimated to $\pm$ 2 K, but it concerns the absolute values only and the relative variations of the brightness temperatures on the disk of the planet on a given image are not affected. The situation is much better for the night of July 27, which had a rather good stability, and the uncertainty of the *absolute* brightness temperatures have been measured to be -0.5/+0.7 K in the worst case (7.93 μm). The signal-to-noise ratio achieved for the images gives an uncertainty on the *relative* temperature measurements of 0.4 K in the worst case (images at 7.93 μm on July 26) and 0.1 K for most of the images recorded at 11.36, 12.18 and 13.33 μm. A selection of images is given on Figure 1, whose main characteristics and brightness temperature contrasts measured on the impact site complexes are summarized in Table 1.

The 9 images of Figure 1a have all been taken on July 25. The first 6 images of Figure 1b have been recorded on July 26 (02:31, 03:17, 03:34, 04:04, 04:22 and 04:52 UT), while the 3 last images (04:18, 04:54 and 05:02

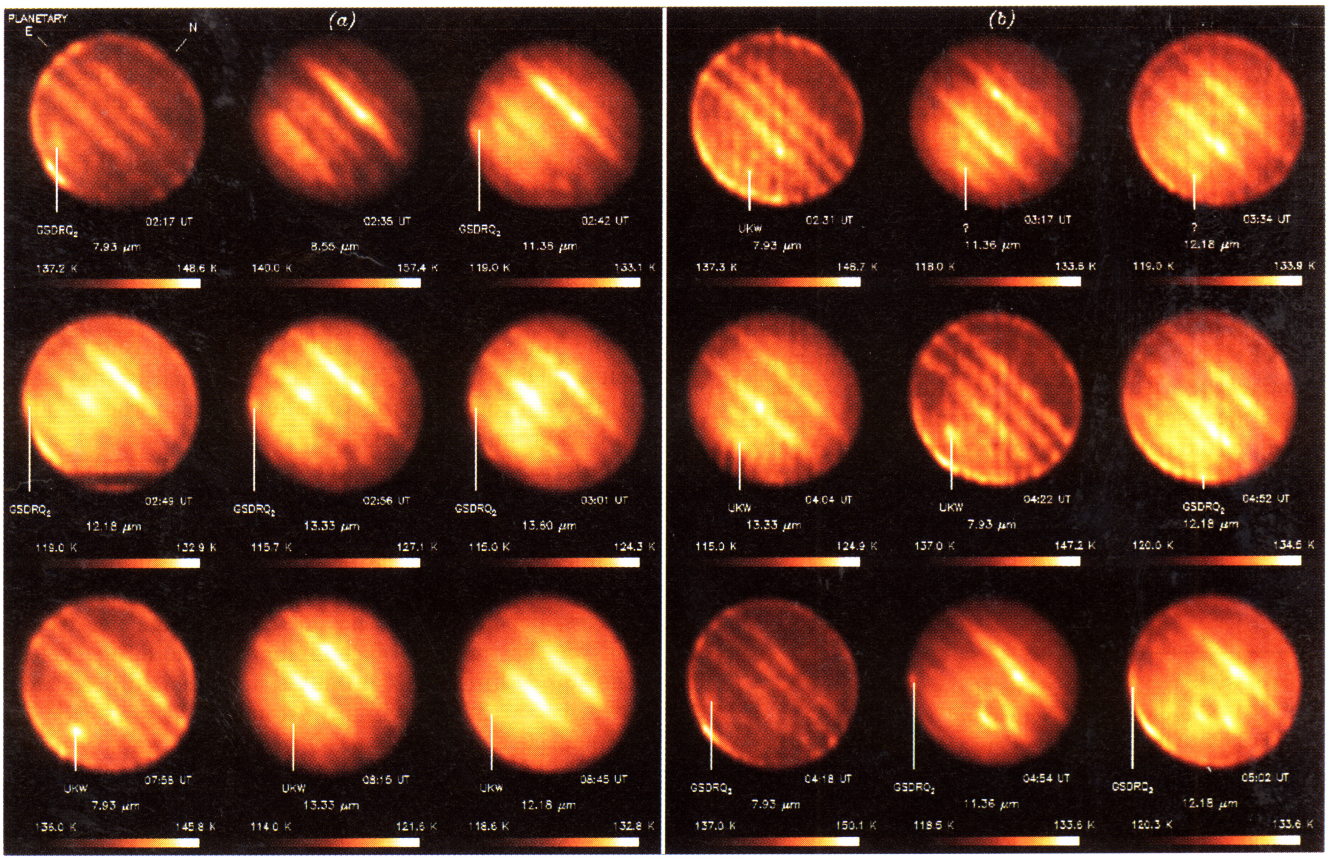

Figure 1. Images of Jupiter recorded on July 25, 26 and 27 at various CVF wavelengths. First plate (from left to right and top to bottom): images recorded on July 25 at 7.93 μm (02:17 UT), 8.55 μm (02:35 UT), 11.36 μm (02:42 UT), 12.18 μm (02:49 UT), 13.33 μm (02:56 UT), 13.60 μm (03:01 UT), 7.93 μm (07:58 UT), 13.33 μm (08:15 UT) and 12.18 μm (08:45 UT). Second plate: images recorded on July 26 at 7.93 μm (02:31 UT), 11.36 μm (03:17 UT), 12.18 μm (03:34 UT), 13.33 μm (04:04 UT), 7.93 μm (04:22 UT) and 12.18 μm (04:52 UT), and on July 27 at 7.93 μm (04:18 UT), 11.36 μm (04:54 UT) and 12.18 μm (05:02 UT).

Table 1. Brightness temperature contrasts between impact site complexes and surrounding areas

Date	Mean Observing Time (UT)	Long. CM ° (Sys III)	Wavelength (μm)	S/N	Visible Site	Location near Limb ?	T_B Contrast (K)
July 25	02:17	64.24	7.93	20	G-S-D-R-Q_2	N	2.0 to 3.6
July 25	02:35	75.12	8.55	30	nothing	–	–
July 25	02:42	79.36	11.36	50	G-S-D-R-Q_2	Y	0.4 to 1.9
July 25	02:49	83.58	12.18	45	"	Y	1.7 to 2.8
July 25	02:56	87.82	13.33	35	"	Y	1.9 to 3.1
July 25	03:01	90.84	13.60	25	"	Y	1.5 to 2.4
July 26	04:52	308.34	12.18	60	"	Y	2.6 to 5.4
July 27	04:18	78.17	7.93	25	"	N	1.9 to 3.3
July 27	04:54	99.93	11.36	65	"	Y	1.9 to 5.4
July 27	05:02	104.77	12.18	70	"	Y	0.8 to 3.7
July 25	07:58	270.39	7.93	20	U-K-W	N	2.6 to 4.8
July 25	08:15	280.67	13.33	20	"	N	0.6 to 1.1
July 25	08:45	298.80	12.18	25	"	N	0.6 to 2.0
July 26	02:31	223.09	7.93	15	"	N	2.4 to 3.3
July 26	03:17	250.90	11.36	55	nothing	–	–
July 26	03:34	261.18	12.18	40	nothing	–	–
July 26	04:04	279.32	13.33	28	U-K-W	N	0.5 to 2.5
July 26	04:22	290.20	7.93	20	"	N	3.4 to 4.9

Main characteristics of the images displayed on figure 1. The visible impact site complex, when any, is given, and its possible location near the limb of the planet is mentionned. The uncertainty on the measured brightness temperature contrasts is 0.4 K in the worst case.

UT) were recorded on July 27. Both sets exhibit the G-S-D-R-Q_2 complex and the U-K-W one at various wavelengths.

From a careful examination of the images and relative brightness temperature measurements obtained (Table 1), we can derive the following conclusions:

i) The highest brightness temperature contrast between the impact sites and the surrounding areas of the planet are provided by the images at 7.93 μm. On the July 25 images, the contrast seems obviously higher on the U-K-W spot than on the G-S-D-R-Q_2 one, as indicated by the fact that the U-K-W spot is the brightest feature on the disk of the planet on the image taken at 07:58 UT, while the brightest spot is on the southern auroral zone on the image taken at 02:17 UT. This can be interpreted by the fact that the U-K-W site is probably dominated by the W impact, which is the "freshest" one, while the G, S, D, R and Q_2 ones are all "old" impacts. It is also likely that the differences in their impacting amplitude play a role, as well as how they affected the levels involved in the emissions at these wavelengths.

ii) There is an obvious decrease of the relative contrast on the U-K-W impact site at 7.93 μm between July 25 (2.6 to 4.8 K) and July 26 (2.4 to 3.3 K), which probably gives an indication on the cooling of the atmospheric levels probed at this wavelength.

iii) Nothing is clearly visible at 8.55 μm. As 8.55 μm is probably, among the wavelengths we had chosen, the one which probes the deepest, this could indicate either that the corresponding atmospheric levels were not perturbed by these impacts, or rather that the perturbation was weak or did not remain long enough to be detectable at this wavelength (0.5 to 1 bar) three days after the last impact. This last hypothesis is probably more realistic, as other observations indicate that the ammonia cloud near 0.5 bar has been reached, as indicated by the detection of stratospheric ammonia emissions (Livengood et al., 1994; Orton et al., 1994; Kostiuk et al., 1994; Griffith et al., 1994; Gierash et al., 1994; Betz et al., 1994).

iv) The impact sites are obviously detected more easily when they are located near the limb of the planet rather than when near the central meridian. This is probably due to the fact that, within a given wavelength range, we probe higher on the limb of the planetary disk than on its center. This would then favour the emissions coming from the G-S-D-R-Q_2 site (almost always near the limb on our images), as compared to the ones coming from the U-K-W site (always near the center of the planet).

v) The contrasts are rather better at 11.36 and 13.33 μm than at 12.18 and 13.33 μm, although these wavelengths are supposed to probe deeper in the atmosphere. An explanation of this could be that the images at 11.36 and 13.33 μm are more affected by the presence of ammonia in the stratosphere, as these wavelengths are more sensitive to ammonia emissions.

Conclusion

We have measured absolute brightness temperatures as well as brightness temperature contrasts at 6 different wavelengths on July 25, 26 and 27. A preliminary analysis of the data indicates that the brightness

temperature contrast between the two observed impact sites (G-S-D-R-Q_2 and U-K-W) and the surrounding areas is of the order of 2 to 5 K, depending on the wavelength and the time after the impacts. Our observations show that the highest contrasts on the impacts are seen (1) on the more recent impacts (U-K-W), as compared to older impacts (G-S-D-R-Q_2); (2) at the wavelengths of 7.93 μm (methane), and 11.36 and 13.33 μm (ammonia); (3) at the limb rather than at central meridian. Points (2) and (3) are understandable, in particular for the methane emission at 7.93 μm, if the stratospheric perturbation is a thermal enhancement of the upper stratosphere, this wavelength peaking higher in the stratosphere than, for example, the continuum wavelength at 8.55 μm. Thermal variation, either by a few degrees over a large altitude range, or by a larger temperature difference in a limited range of altitude in the upper atmosphere, as detailed in Drossart et al. 1993, can produce such brightness temperature variations. A more detailed study of the features and temperatures obtained is in progress.

References

Betz A.L. et al., Stratospheric ammonia in Jupiter as a result of comet SL-9, Bull. Amer. Astron. Soc. **26**, 1590, 1994.

Drossart P. et al., Thermal Profiles in the Auroral Regions of Jupiter, J. Geophys. Res.**98**, NO E10, 18803, 1993.

Gierasch P. et al., A physical interpretation of the SL9 impacts observed from Palomar,Bull. Amer. Astron. Soc. **26**, 1585, 1994.

Griffith C.A. et al., Mid-IR spectroscopy and ammonia images of K impact sites, *Bull. Amer. Astron. Soc.* **26**, 1584, 1994.

Gurwell M.A. et al., Millimeter imaging of the comet P/Shoemaker-Levy 9 impacts on Jupiter, *Bull. Amer. Astron. Soc.* **26**, 1583, 1994.

Kostiuk T. et al., Very high resolution spectroscopy of the Jovian stratosphere in the wake of the SL9 impacts, *Bull. Amer. Astron. Soc.* **26**, 1584, 1994.

Kunde V et al., The tropospheric gas composition of Jupiter's north equatorial belt (NH_3, PH_3, CH_3D, GeH_4 and H_2O) and the jovian D/H isotopic ratio, Astrophys. J.**263**, 443, 1982.

Livengood T. et al., Thermal infrared imaging of the SL9 impact sites using TIMMI at the European Southern Observatory, *Bull. Amer. Astron. Soc.* **26**, 1578, 1994.

Lognonné P. et al., Excitation of Jovian Seismic Waves by the Shoemaker-Levy 9 Cometary Impact, *Icarus* **110**, 180, 1994.

Orton G et al., Jovian atmospheric structure investigation in the NASA IRTF SL9 campaign, *Bull. Amer. Astron. Soc.* **26**, 1584, 1994.

F. Billebaud, Space Science Department of the European Space Agency, ESTEC, NL-2200 AG Noordwijk, The Netherlands

(received December 7, 1994; revised March 28, 1995; accepted March 31, 1995.)